INSPECTION OF SURFACE DEFECTS USING OPTIMAL FIR FILTERS

Ajay Kumar
Department of Computer Science
Hong Kong University of Science & Technology
E-mail: *ajaykr@cs.ust.hk*

ABSTRACT

A new method of surface inspection for the textured materials is investigated. The linear FIR filters that offer optimal energy separation between the defect and defect-free regions of texture have been utilized. Performance of different feature separation criterion with reference to fabric defects has been evaluated. The issues relating to the design of optimal filters for supervised and unsupervised web inspection are discussed. A general web inspection system based on the optimal filters is proposed. The experiments on this new approach have yielded excellent results. The on-line computational simplicity using the proposed scheme confirms the usefulness of the approach for industrial inspection.

1. INTRODUCTION

One of the key factors in the quality assurance of industrial textured materials is the surface inspection. Traditional manual inspection is labor- and cost-intensive and offers major bottleneck in the high-speed production lines. The advantages of automated visual inspection are well known; repeatability, reliability and accuracy.

The design of optimal Gabor filters and wavelets for the inspection of textile defects has been detailed in [1]-[2]. However, the Gabor filters, wavelets and the infinite impulse response (IIR) filters are the filters with only a few free parameters and therefore the search space for optimization is very restricted. Better optimization results can be obtained when the number of free available parameters of a filter is large. A general finite impulse response filter (FIR) has generally more free parameters than an IIR or a Gabor filter. The single biggest advantage of FIR filters is that they can implement any impulse response, provided it is of finite length. The method used in this paper [3] uses closed-form optimal solution derived from the texture model, unlike iterative loop optimization in [1]-[2], and therefore the designed filters are compact and computationally simpler to design. The simplicity of these spatial filters is very attractive for many real-time web inspection problems where large volume of image data has to be processed at high speed.

A survey of several techniques available for the inspection of textured surfaces can be found in [3]. In this paper, it is assumed that every texture, *i.e*. with- or without-defects, can be modeled by using its 2D autocorrelation function. The linear FIR filters that guarantee optimal *discrimination* of energy in local regions rather than optimal *representation* are used in this work. These optimal filters cannot explicitly detect the defects but can make the detection an easier task by greatly attenuating pixel value in the defect-free region relative to regions having defects.

2. STATISTICAL TEXTURE MODEL

The feature extraction model [4] used to design the optimal filter is illustrated in figure 1. The objective of the optimal filter $h_{op}(x,y)$ is to extract those frequencies where the defect-free texture has low signal energy and the texture with defect has high signal energy. In this model, it is assumed that the textures being modeled are wide sense stationary, and that they can be well described by their autocorrelation functions [5]. Let x and y be the spatial indices of acquired image $I(x,y)$ which is filtered by the filter $h_{op}(x,y)$ to generate a new image $w(x,y)$.

$$w(x,y) = \sum_{m=0}^{M-1}\sum_{n=0}^{N-1} h_{op}(m,n)\, I(x-m, y-n) \qquad (1)$$

where $M \times N$ is the size of optimal filter to be designed. For every pixel in $w(x,y)$, the output can be rewritten as

$$w(x,y) = \mathbf{h}_{op}^{T}\mathbf{i}(x,y) \qquad (2)$$

where $\mathbf{h}_{op}$ and $\mathbf{i}(x,y)$ are the vectors of length $Z = M \times N$, obtained by lexicographical ordering of columns of $h_{op}(x,y)$ and $M \times N$ window of $I(x,y)$ around pixel (x,y) respectively. The squaring nonlinear operator $|.|^2$ computes the energy of every pixel in the filtered image $w(x,y)$.

$$s(x,y) = w^2(x,y) \qquad (3)$$

The energy of pixels in (3) is computed in a local region, the size of which is determined by the bandwidth of smoothing filter.

2.1. The Feature mean and variance

The mean value of the feature image $f(x,y)$ can be derived as follows [4]:

$$\mu_f = E\{f(x,y)\} = E\{s(x,y) * g(x,y)\} \quad (4)$$

The smoothing filter $g(x,y)$ is a unity gain low pass filter. Therefore, the mean feature value at the output of this filter is equal to mean feature value at the input. Assuming that the filter coefficients are such that $\sum_{x,y} g(x,y) = 1$, equation (4) can be written as

$$\begin{aligned}\mu_f &= E\{w^2(x,y)\} = E\{(\mathbf{h}_{op}^T\mathbf{i}(x,y))(\mathbf{h}_{op}^T\mathbf{i}(x,y))\} \\ &= \mathbf{h}_{op}^T E\{\mathbf{i}(x,y)\mathbf{i}^{\mathbf{T}}(x,y)\}\mathbf{h}_{op}\end{aligned} \quad (5)$$

defining

$$\mathbf{R}_{ii} = E\{\mathbf{i}(x,y)\,\mathbf{i}^T(x,y)\} \quad (6)$$

equation (5) can be written as

$$\mu_f = \mathbf{h}_{op}^T \mathbf{R}_{ii} \mathbf{h}_{op} \quad (7)$$

where $\mathbf{R}_{ii}$ is the autocorrelation matrix of the image $\mathbf{i}(x,y)$. Since the $\mathbf{R}_{ii}$ in equation (6) is symmetric, the derivative of mean feature value μ_f is given by

$$\frac{\partial \mu_f}{\partial \mathbf{h}_{op}} = \frac{\partial(\mathbf{h}_{op}^T \mathbf{R}_{ii} \mathbf{h}_{op})}{\partial \mathbf{h}_{o\mathbf{p}}} = 2\mathbf{R}_{ii}\mathbf{h}_{op}. \quad (8)$$

Equation (7) and (8) will be used for *closed-form* optimization in section 3. The variance of the feature image $f(x,y)$ is given by

$$\begin{aligned}\sigma_f^2 &= E\{(\mathbf{g}^T\mathbf{s}(x,y))(\mathbf{g}^T\mathbf{s}(x,y))\} - \mu_f^2 \\ &= \mathbf{g}^T\mathbf{R}_{ss}\mathbf{g} - \mu_f^2\end{aligned} \quad (9)$$

where $\mathbf{R}_{ss} = E\{\mathbf{s}(x,y)\mathbf{s}^T(x,y)\}$ is Z × Z autocorrelation matrix which can be readily constructed from the autocorrelation function of image $s(x,y)$.

3. CLOSED-FORM OPTIMIZATION

The expected response of optimal filter to the image with textured defects is strong, *i.e.*, high μ_{f_d}. On the other hand, when a defect-free textured image is presented to this optimal filter, its response should be low, *i.e.*, low μ_{f_r}. *Mahalanobis and Singh* [5] have used the ratio between the average feature values as the cost function.

$$J_1(\mathbf{h}_{op}) = \frac{\mu_{f_d}}{\mu_{f_r}} = \frac{\mathbf{h}_{op}^T \mathbf{R}_{ii_d} \mathbf{h}_{op}}{\mathbf{h}_{op}^T \mathbf{R}_{ii_r} \mathbf{h}_{op}} \quad (10)$$

The optimal solution for (10) is found by setting the gradient of $J_1(\mathbf{h}_{op})$ to zero and using (7)-(8) to obtain the following equation.

$$\mathbf{R}_{ii_r}^{-1}\mathbf{R}_{ii_d}\mathbf{h}_{op} = \psi.\mathbf{h}_{op} \quad (11)$$

where ψ is equal to the object function being optimized, *i.e.*, $J_1(\mathbf{h}_{op})$. Equation (11) is an eigenvalue equation where the filter $\mathbf{h}_{op}$ is the eigenvector and ψ is the eigenvalue. Therefore, the desired optimal filter is the eigenvector $\mathbf{h}_{op}$ that yields maximum object function $J_1(\mathbf{h}_{op})$.

$$J_2(\mathbf{h}_{op}) = \frac{(\mu_{f_d} - \mu_{f_r})^2}{\mu_{f_d}\mu_{f_r}},\ J_3(\mathbf{h}_{op}) = \frac{(\mu_{f_d} - \mu_{f_r})^2}{\sigma_{f_d}^2 + \sigma_{f_r}^2} \quad (12)$$

The design of optimal filters with respect to object function $J_2(\mathbf{h}_{op})$ or $J_3(\mathbf{h}_{op})$, using *closed-form* solution, is similar and has been detailed in [4].

4. FILTER DESIGN SUMMARY

In summary, the optimal filters corresponding to object function $J_1(\mathbf{h}_{op})$, $J_2(\mathbf{h}_{op})$, or $J_3(\mathbf{h}_{op})$ is designed as follows:

(i) The correlation matrices $\mathbf{R}_{ii_r}$ and $\mathbf{R}_{ii_d}$ from fabric samples are computed.
(ii) The eigenvectors of ($\mathbf{R}_{ii_r}^{-1}\mathbf{R}_{ii_d}$) are computed.
(iii) The eigenvector yielding maximum object function ($J_1(\mathbf{h}_{op})$, $J_2(\mathbf{h}_{op})$, or $J_3(\mathbf{h}_{op})$)is selected, and
(iv) Optimal filter $h_{op}(x,y)$ is obtained from elements of $\mathbf{h}_{op}$, by inverse lexicographical reordering.

5. EXPERIMENTS

The proposed scheme was evaluated on the images captured from the real fabric samples. These image samples have been acquired under backlighting condition and covered 1.28 × 1.28 inch^2 area of fabric [3]. The acquired images were digitized into 256 × 256 pixels, with eight-bit resolution. A Gaussian low pass filter, with $f_0 = 1/8$ [6], was used for smoothing. The spatial extent of this filter was empirically fixed as 11×11.

The fabric defects in each of the gathered images are localized in a small region, *i.e.* they are not global. If the complete 256 × 256 pixels image is utilized for designing the optimal filter, the discriminating effect of defect from its large defect-free background diminishes due to the inherent averaging that takes place while computing its correlation matrix $\mathbf{R}_{ii_d}$. Furthermore, the computational time for computing these correlation matrices for the complete image is significantly high. Therefore, only a small image pitch from the region of image having defect (and equal sized image pitch from a defect-free image) is utilized for designing optimal filters. The size of this image pitch is empirically determined, and it depends on the spatial extent of the defect in an image.

6. RESULTS

The experimental results from the proposed defect detection scheme were excellent and few of these are reproduced here. Figure 2 (a) shows the sample of a twill weave fabric with the defect commonly referred to as *mispick*. Using $J_1(\mathbf{h}_{op})$ as the object function, a 7 × 7 optimal filter was designed to segment this defect. Figure

2 (e) shows the magnitude frequency response of this optimal filter. It can be seen that the magnitude frequency response exhibits passbands where local energy estimate is high (corresponding to defect) and stopbands elsewhere. The filtered image is shown in figure 2 (b). As seen from this image, the standard deviation of individual pixels corresponding to defect is much higher than those due to defect-free region and therefore defect can be segmented by any two class linear discriminant function, typically thresholding. The local energy estimate for the image in figure 2 (c) is shown in figure 2 (f). Since the average local energy for region corresponding to defect is 4.419 times (greater than one) that of defect-free region, the defect can be easily be segmented by simple thresholding as shown in figure 2 (d). The optimal filters designed in this experiments were found to be robust and have successfully detected defects of similar nature lying anywhere in the image under inspection. The magnitude of the three object functions, *i.e*. $J_1(\mathbf{h}_{op})$, $J_2(\mathbf{h}_{op})$, $J_3(\mathbf{h}_{op})$, for the different optimal filter size ($M \times N$), for the defect in image 2 (a), is shown in table 1. With the increase in mask size from 3×3 to 19×19, the maximum eigenvalue of equation (11) or the object function $J_1(\mathbf{h}_{op})$ increases linearly. The high magnitude of $J_1(\mathbf{h}_{op})$ results in higher attenuation of the defect-free region relative to the region having defect, but is computationally expansive.

The figure 3 shows that results from the 3×3 optimal filters designed to detect same defect in figure 2(a). The robustness of this 3×3 filter for the detection of other defects is illustrated in figure 3. Due to the nature of weaving process, majority of the defects on the textile web occurs along two directions *i.e*. horizontal (h1) and vertical (h2). Therefore only two optimal filters that can detect *mispick* like defect in two respective directions have been utilized for the web inspection. In this scheme the two local energy estimate from the two filters are added and the resultant image is binarized. The two-filter scheme is computationally simpler and is quite successful as can be seen from results in figure 4 and 5.

7. CONCLUSIONS

In this paper, a new approach for the detection of textured defects using linear FIR filters with optimized energy separation has been investigated. The optimized filters designed to detect a class of defects were robust and successful as long as the defect-free background of texture does not change. One of the important conclusions of this work [3] is that the size of optimal filters has appreciable effect on the defect detection performance. The test conducted on different types of defect and different styles of fabric has yielded promising results. The optimal filters suggested in this work can also be used to supplement the performance of existing system that fail to detect a class of specific defects.

8. REFERENCES

[1] A. Bodnarova, M. Bennamoun and S. Latham "Optimal Gabor filters for textile flaw detection", *Pattern Recogn.*, vol. 35, pp. 2973-2991, Dec. 2002.

[2] W. J. Jasper, S.J. Garnier, and H. Potapalli, "Texture characterization and defect detection using adaptive wavelets," *Opt. Eng.,* vol. 35, pp. 3140-3149, Nov. 1996.

[3] A. Kumar, Automated defect detection in textured materials, Ph.D. Thesis, Department of Elect. & Electr. Engr., The University of Hong Kong, May 2001.

[4] T. Randen and J. H. Husøy, "Texture segmentation using filters with optimized energy separation," *IEEE Trans. Image Process*., vol. 8, pp. 571-582, Apr. 1999.

[5] A. Mahalanobis and H. Singh, "Application of correlation filters for texture recognition," *Appl. Opt*., vol. 33, pp. 2173-2179, Apr. 1994.

[6] A. K. Jain and F. Furrokhnia, "Unsupervised texture segmentation using Gabor filters," *Pattern Recogn.,* vol. 23, pp. 1167-1186, Dec. 1991.

Table 1: Maximum object function as a function of mask size for the *mispick* shown in figure 2(a).

Optimal filter Mask size	$J_1(\mathbf{h}_{op})$	$J_2(\mathbf{h}_{op})$	$J_3(\mathbf{h}_{op})$
3×3	1.4082	0.1183	0.4063
5×5	2.8315	1.1846	1.0283
7×7	4.4187	2.6450	0.9406
9×9	5.5855	3.7645	1.0117
11×11	6.6410	4.7916	1.0602
13×13	7.8826	6.0094	0.9269
15×15	8.8267	6.9399	1.1859
17×17	9.8922	7.9932	1.6401
19×19	10.8588	8.9509	1.3436

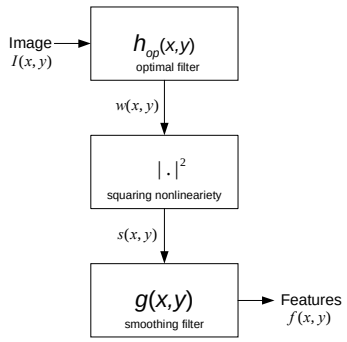

Figure 1: Block diagram of the feature extraction model.

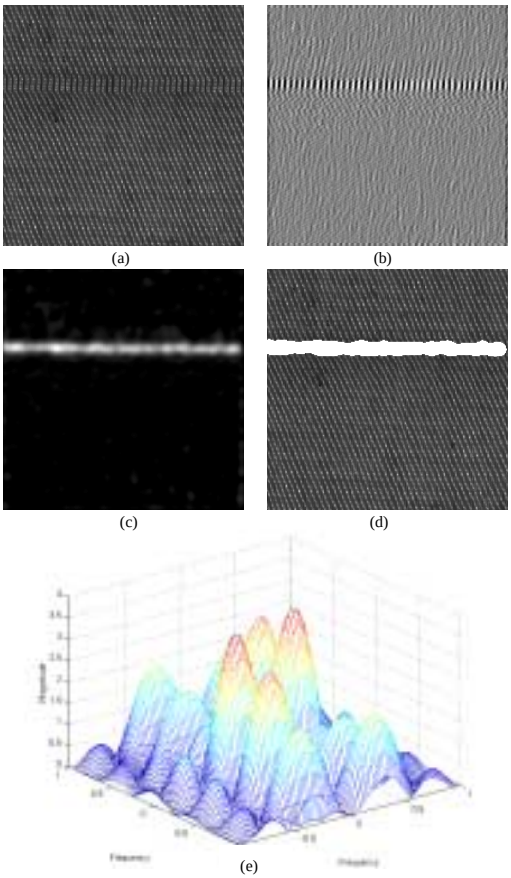

Figure 2: **(a)** Fabric sample with *mispick*, **(b)** after filtering with 7 × 7 optimal filter, **(c)** local energy estimate of image in **(b)**, **(d)** segmented defect after thresholding image **(c)**, **(e)** amplitude frequency response of the optimal filter.

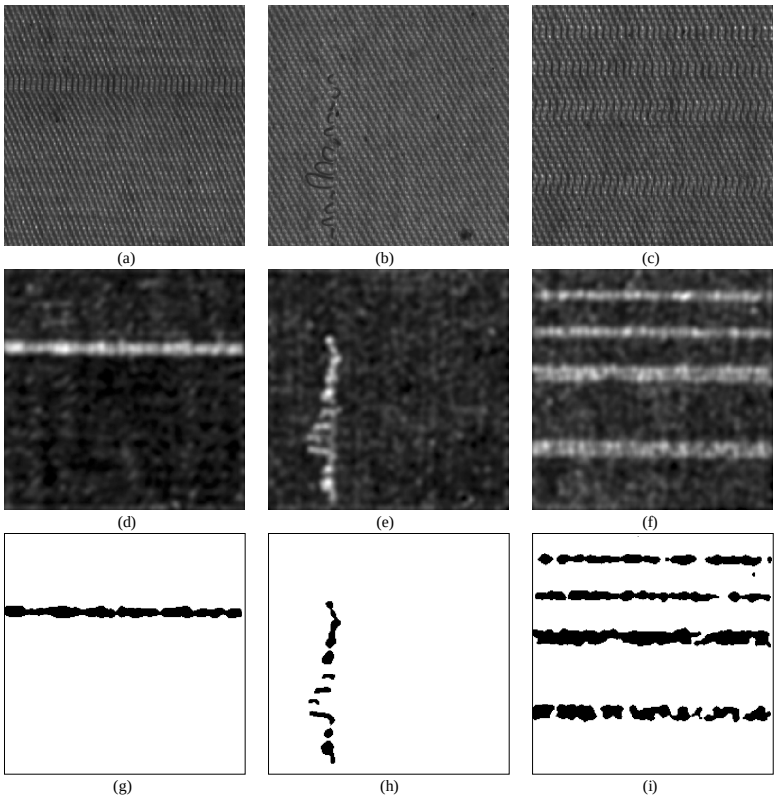

Figure 3: Fabric defects detected with 3 × 3 masks designed to detect *mispick* in figure 2(a), **(a)-(c)** image samples, **(d)-(f)** local energy estimates, **(g)-(i)** segmented defects after thresholding.

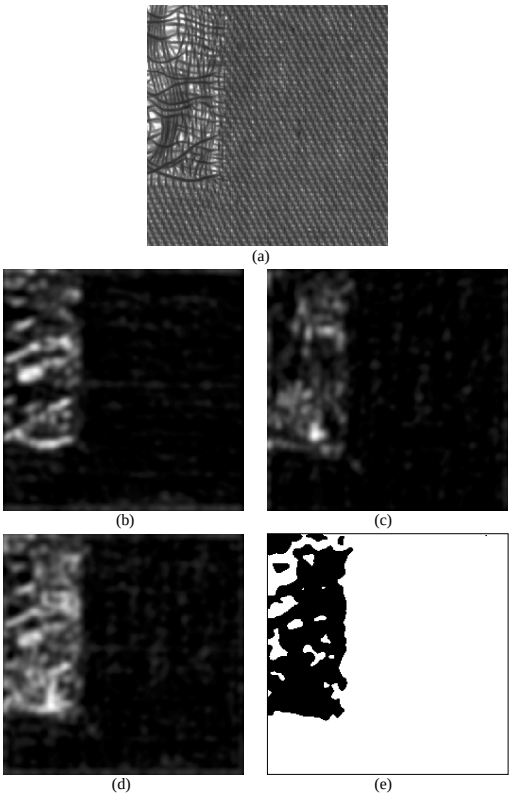

Figure 4: **(a)** Fabric sample with defect, **(b)** output from h1 filter, **(c)** output from h2 filter, **(c)** combined output from h1 and h2 and, **(e)** segmented defect after thresholding image (d).

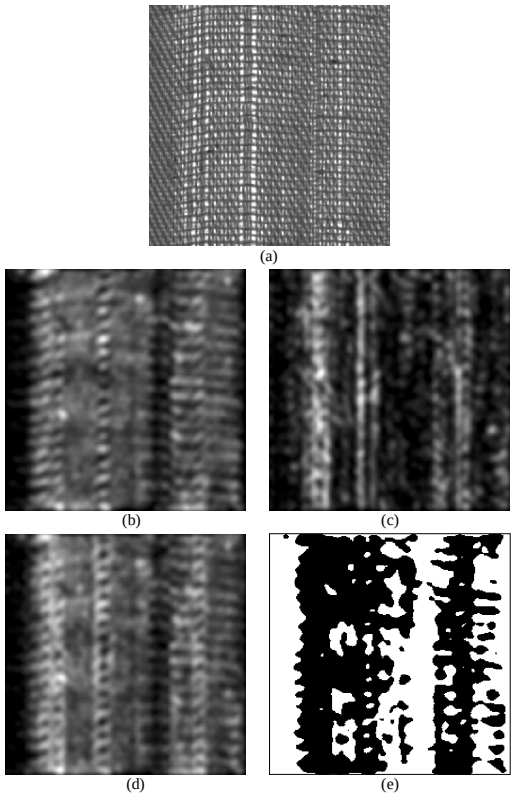

Figure 5: **(a)** Fabric sample with defect, **(b)** output from h1 filter, **(c)** output from h2 filter, **(c)** combined output from h1 and h2 and, **(e)** segmented defect after thresholding image (d).